Conditional Moment Closure With a Progress Variable Approach

Harry Lehtiniemi*[1], Anders Borg[1], and Fabian Mauss[2]

[1] *Lund Combustion Engineering – LOGE AB, Scheelevägen 17, SE-22370 Lund, Sweden*
[2] *Thermodynamics and Thermal Process Engineering, Brandenburg University of Technology, Siemens-Halske-Ring 8, DE-03046 Cottbus, Germany*

Key Words: CMC, Progress variable, Tabulated chemistry, Combustion, CFD

ABSTRACT

A method has been developed that allows for performing reactive flow simulations using conditional moment closure (CMC) without spatial dimension reduction of the CMC grid. The CMC is performed for a progress variable and the emission scalars, using a progress variable parameterization of the combustion chemistry. The method has been implemented into a CFD software package. The proposed method has been tested for a simple spray bomb case, n-heptane spray injection into a constant volume vessel, and compared with the interactive flamelet model.

INTRODUCTION

One of the challenges in turbulent combustion modeling is the closure of the chemical source term. The capacity of today's computers is not allowing for performing Direct Numerical Simulations (DNS) resolving all relevant time- and length scales associated with turbulence, spray, and combustion chemistry at an affordable simulation time scale. Therefore, not all time- and length scales are resolved in industrial CFD simulations, and appropriate closures of terms resulting from averaging procedures are required. Here the discussion is restricted to treatment of the reactive scalars and the chemical source term in the context of Reynolds-averaged Navier-Stokes (RANS) simulations.

The problem with the closure of the chemical source term lies in the difficulty to treat the effect that turbulence fluctuations of the reactive scalars and state variables have on the chemical reaction rates. Approximating the chemical source term using cell mean quantities may cause a deviation in ignition, combustion, and emission prediction between experiments and simulations, due to the exponential nature of the reaction rates. Two main modeling approaches have been developed in the past, attempting to overcome this difficulty: models based on a presumed Probability Density Function (pdf), and models based on transported pdf, see e.g. [1]. The CMC and flamelet models belong to the class of presumed pdf models. In a non-premixed combustion setting the presumed pdf formulation is based on having a solution of the first two moments (mean and variance) of a passive scalar, the mixture fraction. The pdf, used when computing the reactive scalars, is usually a beta pdf.

Our purpose is to present a method for performing a conditional moment closure for a progress variable and emission scalars (soot) on the same grid as used by the flow solver. This work is motivated by the need for model development for emerging direct injection combustion concepts where the ignition timing is not solely controlled by start of injection, but also by the amount of dilution in the combustion chamber and reactivity of the fuel. It may be suspected that local turbulence and scalar fluctuations affect the ignition, combustion, and emission formation phenomena under such operating conditions. Further, in order to be industrially applicable, the complexity and the costs of solving the combustion chemistry need to be kept as low as possible. Therefore the method presented herein builds on a progress variable based parameterization of the chemistry, and tabulation of the transient flamelet ignition process [2],[3]. The proposed method, LTIF-CMC (library of transient tabulated flamelets-CMC) has been implemented using user coding into the commercial CFD software package STAR-CD [4], and a first test of the method has been carried out simulating a constant volume spray bomb case. We compare the results obtained with the proposed method, with results obtained using the interactive flamelet method.

We do not intend to give a full background to neither the flamelet model nor the conditional moment closure model. The flamelet model is detailed by Peters in [1],[5], and the development of the conditional moment closure model has been reviewed by Klimenko and Bilger [6], and recently by Kronenburg and Mastorakos [7]. The relation between the conditional moment closure model and the flamelet model was investigated by Klimenko [8]. It is noted, that when applied for non-premixed combustion, both the flamelet model and the CMC model utilize a passive scalar, the mixture fraction – and

the scalar dissipation rate – as key elements of the model formulation. Moreover, the unconditional averages of the reactive scalars are computed knowing the mixture fraction pdf in both models.

The interactive flamelet model has been applied in studies of spray combustion previously, e.g. by Pitsch et al. [9] in the single interactive flamelet formulation, and by Magnusson et al. [10] using multiple interactive flamelets. Magnusson et al. highlighted that the number of interactive flamelets required to capture the flame lift-off location depends on the operating condition, and that multiple flamelets are required to obtain realistic results when simulating diesel spray combustion using the flamelet model. The multiple representative interactive flamelet (RIF) were first introduced in simulations of e.g. diesel engines by Barths et al. [11], resulting in improved emission predictions.

Also the CMC model has been applied in spray combustion studies previously, e.g. by Kim and Huh [12], who employed a first order 2-D CMC formulation to investigate the effect of droplet sources in the mixture fraction variance equation on autoignition timing; Wright et al. [13] investigated numerical techniques, transport terms, and flame propagation, using a first order 2-D CMC formulation. In [14] Wright et al. investigated i.a. the effect of chemistry choice on autoignition timing and the effect of atomization model on autoignition location. Kim and Huh [12] attempted to include the spray terms in the CMC equations while these terms were omitted from both CMC and mixture fraction variance equations in [13] and [14]. Recently, Borghesi et al. [15] investigated rigorously the effect of the spray source term in the mixture fraction variance equation, and Mortensen and Bilger's [16] CMC formulation, which includes spray terms, using first order 2-D CMC. Several n-heptane spray cases with different amount of ambient oxygen concentration were simulated, and it was found that the inclusion of droplet terms mostly affected predictions in locations where evaporation was intense. Very little effect of the spray terms on ignition delay time was found, and the authors reported virtually no effect on flame propagation and anchoring.

All the previously cited studies have been carried out within the Reynolds-Averaged Navier- Stokes (RANS) framework using first order 2-D CMC. Recently, development towards using a Large-Eddy Simulation (LES) approach for CMC with spray was reported by Bottone et al. [17], who employed a first order 1-D CMC formulation to study n-heptane spray autoignition and combustion.

The aforementioned CMC spray simulations all employed first order CMC. De Paola et al. [18] investigated the impact of utilizing a second order CMC formulation on autoignition timing of an n-heptane plume. It was found that the scalar dissipation rate term in the conditional covariance equation is the driving term. In a configuration with rapidly decaying scalar dissipation, the ignition delay time predicted using first order closure differs little from the one predicted with second order closure. The model formulation herein is restricted to first order closure. It has previously been found that the average conditional scalar dissipation rate is indeed decaying in e.g. diesel sprays – although there are local variations. The model proposed here caters for local variations of scalar dissipation.

Soot calculations within the CMC framework have been performed by e.g. Kronenburg et al. [19], Yunardi et al. [20] and Lignell et al. [21]. In those works, some of the discussion concerns differential diffusion effects. In the model proposed here, we follow our work in reference [22] and assume that it is sufficient to account for varying mixture fraction boundaries, and to condition the scalar dissipation rate to the mixture fraction with maximum scalar dissipation. The latter avoids conditioning the scalar dissipation rate to a non-existing mixture fraction, i.e. if the maximum mixture fraction is smaller than the stoichiometric mixture fraction.

We proposed before a soot model, based on a flamelet library of source terms [23], [24]. The work presented here avoids that the mixture fraction dependence of the soot moments needs to be presumed. Instead the development of the profiles for the soot moments is calculated from the CMC equations.

The experimental setup for the test calculations performed here is described in [25],[26].

THE TIF AND LTIF-CMC MODELS

In this section the applied combustion models are described briefly. The interactive flamelet model implementation, TIF, follows the description in [27]. The LTIF-CMC model which constitutes new development, and the approach for table generation is described in more detail than the well-established interactive flamelet model.

Both TIF and LTIF-CMC relies on transport of mixture fraction and mixture fraction variance in the flow-field. The transport equations are detailed in e.g. [1]. No species are transported in the flow-field. Instead the properties required for calculation of thermodynamics and density in the flow-field are calculated from the TIF or LTIF-CMC solution in phase-space and the mixture fraction pdf (here a beta pdf defined by the mixture fraction and its variance).

TIF – Transient Interactive Flamelet Model

The TIF model is an interactive flamelet model. In the flamelet model a turbulent flame is viewed as consisting of an ensemble of laminar flamelets. The main feature of the flamelet model is that it allows for a decoupling of chemistry and flow. A mathematical transform is made from physical space $(\vec{x};t)$ to phase-space $(\xi;\tau)$, allowing for reducing the three-dimensional problem to one dimension. By defining the scalar dissipation rate χ:

$$\chi \equiv 2D_{\xi}(\nabla\xi)^2 \qquad (1)$$

and performing the flamelet transform, the conservation equations for reactive scalars (chemical species) and enthalpy are expressed in flamelet space, assuming unity

Lewis numbers:

$$\rho\frac{\partial Y_i}{\partial \tau}=\frac{\rho\chi}{2}\frac{\partial^2 Y_i}{\partial \xi^2}+\omega_{\mathrm{i}} \quad (2)$$

$$\rho\frac{\partial h}{\partial \tau}=\frac{\rho\chi}{2}\frac{\partial^2 h}{\partial \xi^2}+\frac{dp}{dt}+\dot{q}. \quad (3)$$

The interactive flamelets are solved on-line with the flow. In this work multiple flamelets are used with fuel mass based flamelet splitting, and for each flamelet a probability marker is transported. Since the flamelet splitting is fuel mass based, this transport equation follows a standard passive scalar transport equation with a source term from fuel evaporation. Further details on the TIF model implementation can be found in [27].

Progress variable and chemistry tabulation

Based on previous findings [2],[3] we base our progress variable on chemical enthalpy (enthalpy of formation). This is a quantity which allows for a single variable description of the autoignition process. It is observed that a transport equation for chemical enthalpy can be formulated in physical space. Assuming unity Lewis numbers, and applying the flamelet transform, the following equation is obtained in mixture fraction space for chemical enthalpy:

$$\rho\frac{\partial h_{298}}{\partial t}=\frac{\rho\chi}{2}\frac{\partial^2 h_{298}}{\partial \eta^2}+\rho\omega_{h_{298}}. \quad (4)$$

We have found [3] that it is necessary to use tables based on transient igniting flamelets in order to accurately capture the effect of scalar dissipation on the ignition process.

The generated tables contain the source term for the chemical enthalpy, NASA polynomial coefficients, mean molecular weight, and emission source terms as function of mixture fraction, enthalpy (sum of chemical and thermal enthalpy), pressure, scalar dissipation and the chemical enthalpy itself. Species of interest are also stored in the tables and can be retrieved in a post-process step. Emissions, such as soot and NOx, need to be treated using a source-term approach as the chemistry governing emission formation processes is slow [24]. The skeletal n-heptane mechanism from Zeuch et al. [29] was used.

CMC for the progress variable

The transport equation for the conditionally averaged scalars (progress variable, soot moments) reads, omitting spray terms and terms that have a minor contribution when investigating systems with high Reynolds numbers:

$$\frac{\partial Q_i}{\partial t}+\langle \boldsymbol{v}|\eta\rangle\cdot\nabla Q_i=\frac{\langle\chi|\eta\rangle}{2}\frac{\partial^2 Q_i}{\partial \eta^2}+\langle\omega_i|\eta\rangle+e_y, \quad (5)$$

where the conditionally averaged scalar Q_i is defined as:

$$\rho_\eta Q_i(\vec{x};t,\eta)=\overline{\langle\rho\psi_i(\vec{x},t)|\xi(\vec{x},t)=\eta\rangle}=\overline{\langle\rho\psi_i|\eta\rangle}. \quad (6)$$

The first term on the R.H.S. of Eq. (5) considers diffusive transport in mixture fraction space. This term is closed assuming an inverse complementary error function dependency of scalar dissipation in mixture fraction space, and conditioning the scalar dissipation on the location of maximum scalar dissipation ($\xi_{\max}/2$), assuming an inverse complementary error function shape of scalar dissipation in mixture fraction space. This model is similar to the amplitude mapping closure model (AMC) [28], which is frequently used in CMC modeling.

The source term (second term on the R.H.S. of Eq. (5)) is closed with a first order closure:

$$\langle\omega_i|\eta\rangle=\omega_i(\mathbf{Q},\eta), \quad (7)$$

where **Q** for the progress variable source term consists only of the progress variable – chemical enthalpy – itself, while for the source terms for the soot moment source terms **Q** consists of the progress variable and the soot moments. In a similar manner, for any other emission source term (NOx) the source term is formed based on the progress variable, and the emission scalar. The fluctuation around the conditional mean (third term on the R.H.S. of Eq. (5)) is closed in a simplified manner assuming

$$e_y\approx\nabla\cdot(\langle D_t|\eta\rangle\nabla Q_i), \quad (8)$$

with the conditional turbulent diffusivity taken as

$$\langle D_t|\eta\rangle\approx\frac{\nu_t}{Sc_t} \quad (9)$$

with ν_t computed using the turbulence model. The conditional velocity, appearing in the second term on the L.H.S., is modeled as:

$$\langle\boldsymbol{v}|\eta\rangle\approx\tilde{\boldsymbol{v}}. \quad (10)$$

This formulation allows for using the built-in transport equations for passive scalars in STAR-CD. Eq. (5) is thus solved in an operating-splitting fashion, where the flow solver handles the transport terms in physical space, and a "flamelet" solver handles the transport in mixture fraction space and the source term. The "flamelet" solver is called at the beginning of each CFD time step for every cell. The "flamelet" solver uses an implicit backward-differencing method where the time step is automatically determined.

TEST CALCULATIONS

Test calculations using the proposed LTIF-CMC model and the established TIF model have been performed. Two n-heptane fuelled spray bomb test cases at 21 % and 12 % (vol.) ambient oxygen reported by Idicheria and Pickett [25] were selected as a first test.

The CFD grid is a 6° sector model, 108 x 54 mm with cyclic boundaries. The mesh is non-uniform, using 5832 cells with a cell edge length of around 0.55 mm close to the injector. The cell edge length is increasing with a growth factor towards the vessel walls. Only one cell layer is used in azimuthal direction and thus the grid is essentially a 2-D grid. Turbulence is modeled with the standard $k-\varepsilon$ turbulence model with its default constants. The used STAR-CD spray sub-models [4] are used with

their default STAR-CD constants, and consist of the effective nozzle model; the Reitz atomization model; and the Reitz break-up model. The MARS (Monotone advection and reconstruction) discretization scheme [4] is used for all passive scalars, enthalpy, turbulence, and momentum. No active scalars are transported why user coding for density and enthalpy calculation is used. In the LTIF-CMC calculation the soot particle size distribution is calculated by transporting the conditional averages of the two first moments of the particle size distribution function (PSDF) and the chemical contribution to the soot moment source terms is retrieved from the same table as the progress variable source term. The source term of coagulation is calculated during the execution of the program. In the TIF calculation the moments of the soot particle size distribution function are calculated on-line by the interactive flamelets.

The amount of grid points in mixture fraction space is set to 51. For the LTIF-CMC method this gives 51 transport equations for the progress variable, and 2 x 51 transport equations for the soot moments.

Prior to the LTIF-CMC calculation, transient flamelet tables for the 21 % and 12 % O_2 (vol.) conditions reported in [25] were constructed. Based on previous findings, the tables were constructed for five different scalar dissipation rate levels: 0.1, 1, 10, 100 and 1000 s^{-1}. The nominal ambient temperature is 1000 K, and the nominal ambient density 14.8 kg/m^3, giving a pressure of 4.2 MPa. The level of 12 % O_2 corresponds to a stoichiometric mixture fraction of 0.0361, i.e. approximately 43 % EGR. For the 21 % O_2 case the stoichiometric mixture fraction is 0.0622. The fuel is n-heptane, injected at a constant flow rate for approximately 7 ms through a 0.1 mm nozzle hole.

A mass based splitting is adopted in the TIF calculations. 20 flamelets are used with each flamelet representing 5 % of the injected mass.

RESULTS AND DISCUSSION

Table 1 compares the ignition delay time and the lift-off length with the experimentally determined ones.

Table 1 Experimental and simulated ignition delay times and lift-off length (LOL).

		Ign. delay [ms]	**LOL [mm]**
21 % O_2	Experiment	0.42	17.0
	LTIF-CMC	0.43	17.0
	TIF	0.45	25.0
12 % O_2	Experiment	0.83	29.2
	LTIF-CMC	1.10	32.0
	TIF	1.20	37.5

The experimental ignition delay time was determined through analyzing the pressure trace and applying a speed-of-sound correction to account for the time for the pressure wave to travel from the ignition location to the pressure transducer. For the calculations the location of maximum rate of temperature increase was chosen. Figures 1 and 2 show the maximum calculated temperature in the domain, with the experimental ignition delays denoted by black vertical lines in Fig 2.

The lift-off length was in the experiments determined through OH* chemiluminescence during a time period of 3 ms – 6 ms ASOI. For the calculated lift-off lengths, the flow-fields at 3.5 ms ASOI from respective simulations were investigated. In the calculations the iso-contour of a OH mass fraction of 2.5e-4 was chosen for the 21 % O_2 case as recommended on the ECN website [26]. At 12 % O_2 the recommended limit value is higher than the maximum OH mass fraction in the domain. The threshold value for the 21 % O_2 case corresponds to around 15 % of the maximum OH mass fraction why the lift-off-length in the 12 % O_2 case was based on 15 % of the maximum OH mass fraction in the domain. It is likely that a combustion progress based lift-off threshold is more suitable when comparing lift-off length for different ambient O_2 levels.

For the 21 % O_2 case the LTIF-CMC and TIF calculations are able to quite reasonably reproduce the ignition delay time while for the 12 % O_2 case the ignition delay time is overpredicted. The lift-off length is reasonably predicted by the LTIF-CMC model for both conditions while the TIF simulation overpredicts the lift-off length.

Fig 3 shows the flow-field at 3.5 ms for the 21 % O_2 case. The black iso-contours in the mixture fraction, temperature and soot moment 1 (which can be related to soot mass) plots correspond to $2\xi_{st}$, ξ_{st}, and $\xi_{st}/2$ respectively and the white iso-contours to temperature iso-surfaces of 1700 K and 1200 K respectively. For the OH mass fraction field, the black line corresponds to the ξ_{st} iso-surface, and the white line to the OH mass fraction lift-off threshold value.

Fig 4 shows the flow-field at 3.5 ms for the 12 % O_2 case. The black iso-contours in the mixture fraction, temperature and soot moment 1 plots correspond to $2\xi_{st}$, ξ_{st}, and $\xi_{st}/2$ respectively and the white iso-contours to temperature iso-surfaces of 1400 K and 1200 K respectively. For the OH mass fraction field, the black line corresponds to the ξ_{st} iso-surface, and the white line to the OH mass fraction lift-off threshold value.

It is noted that the most distinct difference between the LTIF-CMC and TIF calculations are in the prediction of the shape of the soot cloud. The soot cloud in the TIF calculation is more diffused than in the LTIF-CMC calculation. The LTIF-CMC method has a higher spatial resolution than the TIF method and it is likely that this causes the differences between the two methods.

CONCLUSION

A method allowing for CMC calculations on the same grid as the flow calculation through the use of a progress variable and tabulated chemistry (LTIF-CMC) has been developed and presented. The method was implemented in a CFD software, and a comparison between the new LTIF-CMC method and the established TIF method was carried out for a simple spray bomb case.

It was found that the LTIF-CMC method predicted

slightly shorter ignition delay than the TIF model. The LTIF-CMC was able to better predict the lift-off length than the TIF model.

NOMENCLATURE

Symbols

D_t	Eddy diffusivity
D_ξ	Mixture fraction diffusion coefficient
e_y	Fluctuation around the conditional mean
h	Chemico-thermal enthalpy
h_{298}	Chemical enthalpy
k	Turbulent kinetic energy
p	Pressure
$\mathbf{Q}$	Vector of conditionally averaged scalars
Q_i	Conditionally averaged scalar i
q	Volumetric heat loss term
Sc_t	Turbulent Schmidt number
t	Time
$\boldsymbol{v}$	Velocity vector
$\vec{x}$	Cartesian coordinate vector
Y	Mass fraction
ε	Turbulent kinetic energy dissipation
η	Mixture fraction sample space variable
v_t	Eddy viscosity
ξ	Mixture fraction
ρ	Density
τ	Flamelet time
χ	Scalar dissipation rate
ψ_i	Scalar i
ω	Source term

Subscripts

h_{298}	Chemical enthalpy
i	Scalar index
max	Maximum
st	Stoichiometric

Operators

$\tilde{}$	Favre average
$\bar{}$	Reynolds average
$\langle \cdot \vert a = b \rangle$	Conditional average

REFERENCES

[1] N. Peters, *Turbulent Combustion*. Cambridge University Press, Cambridge, 2000.

[2] H. Lehtiniemi, F. Mauss, M. Balthasar, and I. Magnusson, *Combust. Sci. and Tech.* 178 (10-11) (2006) 1977-1997.

[3] A. Borg, H. Lehtiniemi, F. Mauss, Poster, Proceedings of ICDERS2011, 23rd International Colloquium on the Dynamics of Explosions and Reactive Systems, UC Irvine, CA, USA, July 24-29, 2011.

[4] CD-adapco group: "STAR-CD 4.16 User Manual", 2011.

[5] N. Peters, *Prog. Energy Combust. Sci.* 10 (3) (1984) 313-339.

[6] A. Y. Klimenko, R. W. Bilger, *Prog. Energy Combust. Sci.* 25 (1999) 595-687.

[7] A. Kronenburg , E. Mastorakos, *In:* T. Echekki and E. Mastorakos (eds.), *Turbulent Combustion Modeling*. *Fluid Mechanics and Its Applications vol. 95*. Springer, New York, 2011, p. 91.

[8] A. Y. Klimenko, *Combust. Theory Modelling* 5 (2001) 275-294.

[9] H. Pitsch, P. Wan, N. Peters: "Numerical investigation of soot formation and oxidation under diesel engine conditions", SAE Technical Paper 952357, 1995.

[10] I. Magnusson, M. Balthasar, T. Hellström, Proceedings of THIESEL 2006, Conference on thermo- and fluid dynamic processes in diesel engines, Valencia, Spain, 2006.

[11] H. Barths, C. Hasse, G. Bikas, N. Peters, *Proc. Combust. Inst.* 28 (2000) 1161-1168.

[12] W. T. Kim, K. Y. Huh, *Proc. Combust. Inst.* 29 (2002) 569-567.

[13] Y. M. Wright, G. De Paola, K. Boulouchos, E. Mastorakos, *Combust. Flame* 143 (2005) 402-419.

[14] Y. M. Wright, O. N. Margari, K. Boulouchos, G. De Paola, E. Mastorakos, *Flow Turbulence Combust.* 84 (1) (2010) 49-78.

[15] G. Borghesi, E. Mastorakos, C. B. Devaud, R. W. Bilger, *Combust. Theory Modelling* 15 (5) (2011) 725-752.

[16] M. Mortensen, R. W. Bilger, *Combust. Flame* 156 (2009) 62-72.

[17] F. Bottone, A. Kronenburg, A. J. Marquis, A. D. Gosman, E. Mastorakos, Proceedings of the European Combustion Meeting, Cardiff, UK, June 2011.

[18] G. De Paola, I. S. Kim, E. Mastorakos, *Flow Turbulence Combust.* 82 (2009) 455-475.

[19] A. Kronenburg, R. W. Bilger, J. H. Kent, *Combust. Flame* 121 (1-2) (2000) 24-40.

[20] Yunardi, R. M. Wolley, M. Fairweather, *Combust. Flame* 152 (3) (2008) 360-376.

[21] D. O. Lignell, J. C. Hewson, J. H. Chen, *Proc. Combust. Inst.* 32 (2009) 1491-1498.

[22] F. Mauss, K. Netzell, H. Lehtiniemi, *Combust. Sci. and Tech.* 178 (2006) 1871-1885.

[23] G. Nakov, F. Mauss, P. Wenzel, R. Steiner, C. Krüger, Y. Zhang, R. Rawat, A. Borg, C. Perlman, K. Fröjd, H. Lehtiniemi, *SAE International Journal of Engines* 2 (2) (2010) 89-104

[24] X.S. Bai, L. Fuchs, M. Balthasar, F. Mauss, *Proc. Combust. Inst.* 27 (1998) 1623-1630

[25] C. A. Idicheria, L. M. Pickett, SAE Technical Paper 2005-01-3834, 2005.

[26] http://www.sandia.gov/ecn/index.php

[27] H. Lehtiniemi, Y. Zhang, R. Rawat, F. Mauss, SAE Technical Paper 2008-01-0957, 2008.

[28] E. E. O'Brien, T.-L. Jiang, *Phys. Fluids A* 3 (12) (1991) 3121-3123.

[29] T. Zeuch, G. Moréac, S. S. Ahmed, F. Mauss, *Combust. Flame* 155 (2008) 651-674.

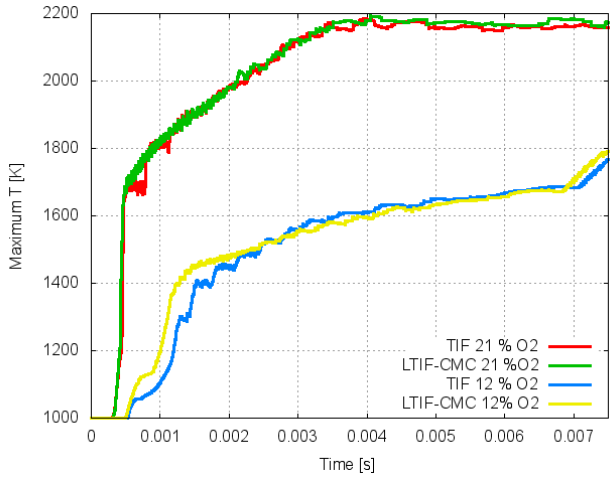

Fig. 1 Maximum temperature for 21 % (vol.) ambient oxygen, red line: TIF, green line: LTIF-CMC; and for 12 % (vol.) ambient oxygen, blue line: TIF, yellow line: LTIF-CMC.

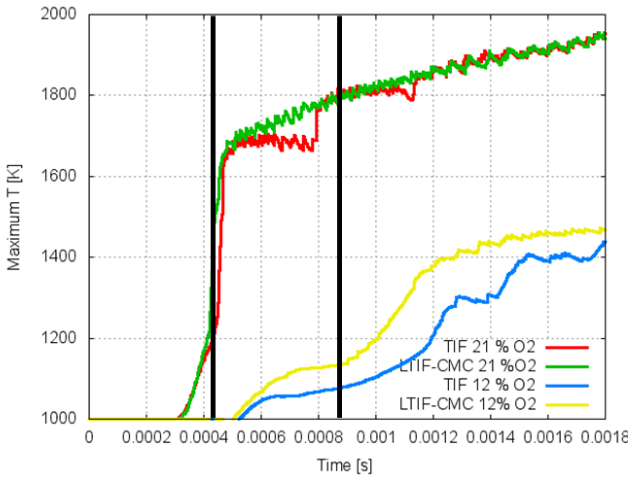

Fig. 2 Experimental ignition delay times marked with black vertical lines. Maximum temperature for 21 % (vol.) ambient oxygen, red line: TIF, green line: LTIF-CMC; and for 12 % (vol.) ambient oxygen, blue line: TIF, yellow line: LTIF-CMC.

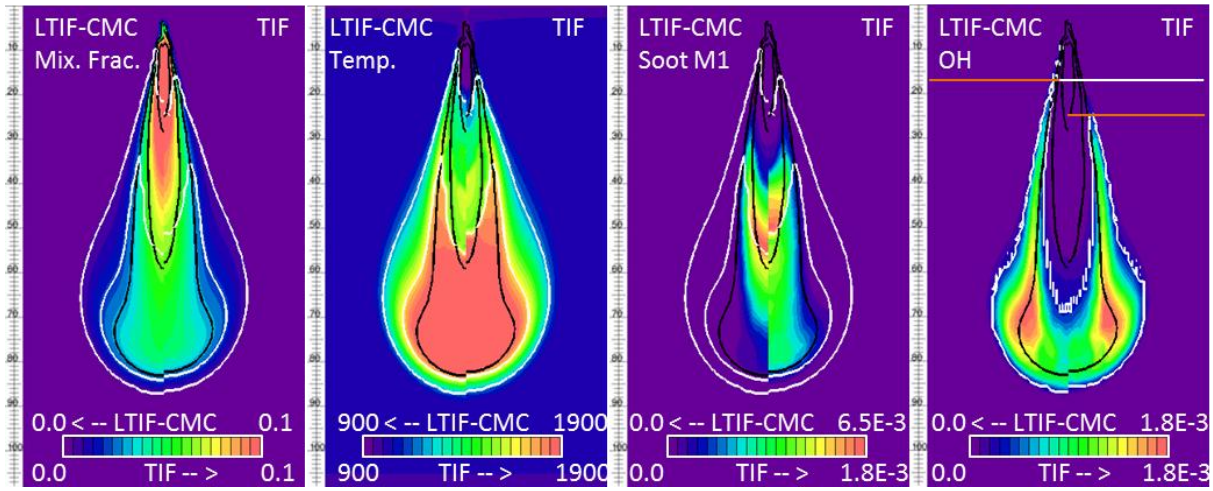

Fig. 3 Contour plots for 21 % (vol.) ambient oxygen at 3.5 ms ASOI for mixture fraction, temperature (K), soot moment 1 (mol/kg) and OH mass fraction. The white horizontal line in the OH plot shows the measured lift-off distance and the red horizontal lines the ones from the simulations. The ruler on the left shows the distance from the nozzle hole in mm.

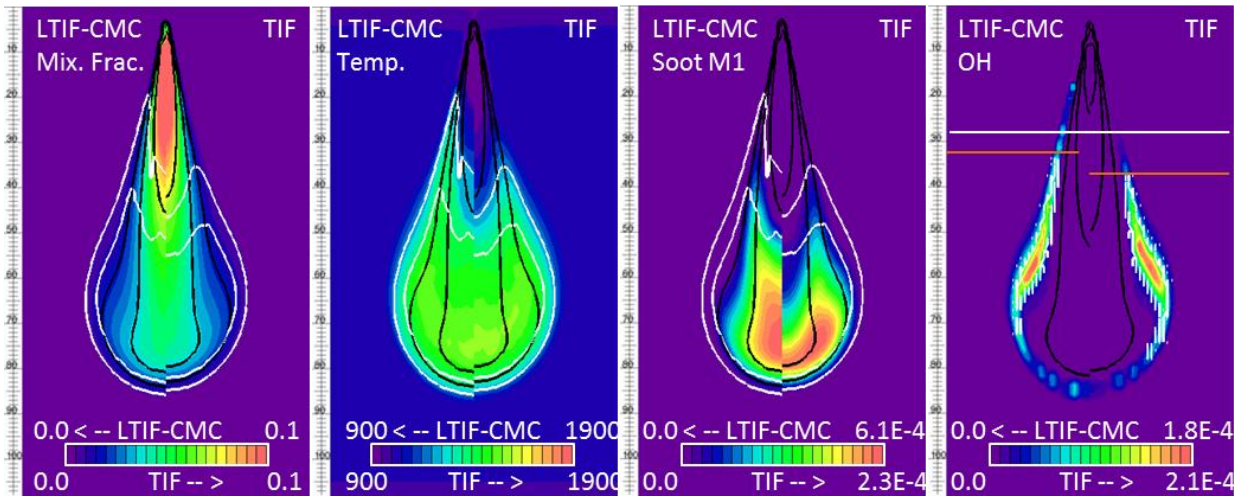

Fig. 4 Contour plots for 21 % (vol.) ambient oxygen at 3.5 ms ASOI for mixture fraction, temperature (K), soot moment 1 (mol/kg) and OH mass fraction. The white horizontal line in the OH plot shows the measured lift-off distance and the red horizontal lines the ones from the simulations. The ruler on the left shows the distance from the nozzle hole in mm.